Molecular Crystals and Liquid Crystals Science and Technology. Section A. Molecular Crystals and Liquid Crystals

Publication details, including instructions for authors and subscription information:
http://www.tandfonline.com/loi/gmcl19

Optical Frederiks Transition: Bulk Director Reoriententation Measurement From Diffraction Pattern and T.I.R Investigations

M. Warenghem [a], M. Ismaili [a], F. Simoni [a b], L. Bloisi [a b] & F. Vicari [a b]

[a] Laboratoire de Dynamique et Structure des Matériaux Moléculaires, U.R.A. C.N.R.S. 801; U.S.T.L.; F.59655, VILLENEUVE D'ASCQ, Cedex

[b] Dipartimento di Scienze Fisiche;, Università di Napoli;, Piazzale Tecchio 80, 80125, NAPOLI, ITALY

Version of record first published: 24 Sep 2006.

To cite this article: M. Warenghem , M. Ismaili , F. Simoni , L. Bloisi & F. Vicari (1994): Optical Frederiks Transition: Bulk Director Reoriententation Measurement From Diffraction Pattern and T.I.R Investigations, Molecular Crystals and Liquid Crystals Science and Technology. Section A. Molecular Crystals and Liquid Crystals, 251:1, 61-72

To link to this article: http://dx.doi.org/10.1080/10587259408027192

Mol. Cryst. Liq. Cryst. 1994, Vol. 251, pp. 61–72
Reprints available directly from the publisher
Photocopying permitted by license only

Printed in the United States of America

OPTICAL FREDERIKS TRANSITION: BULK DIRECTOR REORIENTATION MEASUREMENT FROM DIFFRACTION PATTERN AND T.I.R. INVESTIGATIONS .

M. WARENGHEM, M. ISMAILI, F. SIMONI°, L. BLOISI°, F. VICARI°

Laboratoire de Dynamique et Structure des Matériaux Moléculaires
U.R.A. C.N.R.S. 801; U.S.T.L.; F.59655, VILLENEUVE D'ASCQ Cedex
°Dipartimento di Scienze Fisiche; Università di Napoli; Piazzale Tecchio 80
80125 NAPOLI, ITALY

Abstract Three different results on optically distorded nematic films are presented. They have been derived from T.I.R. experiments and graphical discussion on the observed far field diffraction pattern. First, the optically induced director reorientation profile (radial dependence) in a nematic film can be much more larger than the pump beam profile. Second, a maximum reorientation tilt angle as large as 80 degrees can be obtained and third, the same sample can be focusing, diffracting and defocusing depending on the pump power. The later is a pure thermal effect and occurs as the boundary conditions are very weak.

INTRODUCTION

The photorefractive nature of a nematic film, leading to focusing, diffraction or defocusing, has been extensively studied. This nature is due to either the induced thermal gradient, a collective dielectric reorientation (the so-called Optical Frederiks Transition; O.F.T.) or both[1]. In a first paper[2], the measurement of the local temperature change within the C.W. argon laser pump beam illuminating a homeotropic nematic film under normal incidence has been reported. In addition, the optical field induced director tilt angle on the surface has been deduced and found to depend linearly on the pump power. These measurements have been achieved using total internal reflection (T.I.R., Abbe like setup) experiments. The measurement of the incidence angle that limits the transmission and the total internal reflection regimes yields to the ordinary and extraordinary indices

measurements and therefore respectively to the local temperature and to the surface tilt angle measurements.

This paper deals with the same sample geometry, that is to say a homeotropic nematic film illuminated by a C.W. laser beam under normal incidence. It is reported the optically induced bulk director reorientation measurement using the T.I.R. technique. In addition, the number of diffraction rings have been counted in the far field of the pump beam: it decreases while the pump power is increasing, as once reported[3]. However, in our experiment, as the pump power is large enough, the rings are no longer visible . Using a graphical discussion, this new behavior is shown to be due to the weak anchoring conditions. The discussion also yields to an estimation of the width of the reorientation profile compared with that of the pump beam. In short, the bulk director tilt angle θ depends on both variables r and z: the reflectivity curves allow to determine the z dependence of the function $\theta(r,z)$ for $r = 0$ and the diffraction pattern gives informations on the radial dependence of the function $\theta(r,z)$.

All the results presented in this paper are derived from experiments using the Total Internal Reflection setup and a part of the data processing which have already been described in an other paper in this issue (Ref. 2). This description is therefore skipped here and in the first part, only a further data processing is presented; it allows to obtain the director tilt angle distribution in the bulk. In the second part, the results obtained for the 5CB films are presented and in the third part the far field diffraction pattern is discussed versus the pump power changes.

I. EXPERIMENTAL; data processing.

The leftmost part of a reflectivity curve (as shown in figure 2 of Ref. 2) is an equal thickness fringe pattern and the processing of these data according to the method described in the Ref. 2 gives informations on the nematic film structure, mainly its thickness, the surface director tilt angle and whether or not the film is distorded. As a film is found to be distorded, a more sophisticated processing can be used[4,5]. It allows to obtain the director distribution within the sample without theoretical model. This bulk distorsion determination is shortly presented hereafter; the notations are indicated in figure 1.

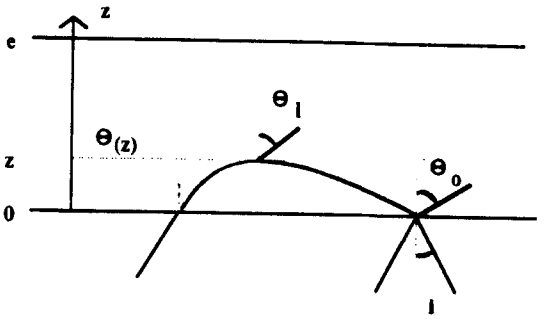

FIGURE 1 Notations used in the phase difference calculation.

We consider the case where the fringe pattern corresponds to the interferences between the beam reflected at the first interface and the transmitted beam which is totally reflected within the sample (Fig. 3b, Ref. 2). The phase difference between the two beams or the order of interference is expressed as below:

$$\frac{\Phi}{2.\pi} = \frac{1}{\lambda}\int_0^z n(\theta,r).\cos(r).dz' + \frac{1}{\lambda}\int_z^0 n(\theta,r').\cos(r').dz' \qquad 1$$

where the first integral corresponds to the part of the transmitted beam going up and the second to that going down, θ and r are respectively the local optical axis tilt angle and local refraction angle with respect to the normal to the interface. The limit of the integral z is a part of the total thickness : it corresponds to the place where the transmitted beam is totally reflected and at that place, the director tilt angle is noted θ_l (Fig. 1). After some algebra, this phase difference looks like the expression 2:

$$\frac{\Phi}{2\pi} = \frac{2.n_e.n_o}{\lambda}\int_{\theta_0}^{\theta_l} \frac{\sqrt{g^2(\theta)-k^2}}{g^2(\theta)} z\,d\theta \qquad 2$$

where g(θ) and k are defined below:

$$g^2(\theta) = n_e^2\cos^2(\theta) + n_o^2\sin^2(\theta)$$
$$k^2 = N^2\sin^2(i) \qquad 3$$

The lower limit θ_0 of the integral 2 is the director tilt angle on the interface (z=0), whereas the upper limit θ_l is defined as below:

$$g^2(\theta_l) = k^2 \qquad 4$$

On the experimental curve, the abscissa i_j of the j^{th} extremum can be measured and using respectively the relations 3 and 4, the associated k_j and θ_j values can be calculated. Remembering that the order of interference is an integer for an extremum of the reflected intensity, the relation 2 is applied to the p^{th} extremum and the integral is split using the different θ_j values calculated as described above, yielding to the relation 5 below:

$$\frac{\Phi_p}{2\pi} = p = \frac{2.n_e.n_o}{\lambda}\sum_{j=0}^{p-1}\left[\int_{\theta_j}^{\theta_{j+1}} \frac{\sqrt{g^2(\theta)-k_p^2}}{g^2(\theta)}\dot{z}\,d\theta\right] \qquad 5$$

Experimentally, the two angles θ_j and θ_{j+1} are very close together and a linear approximation for the function $z(\theta)$ in this range can reasonnably be used. Therefrom, the derivative $\dot{z}$ that comes in the integral can be considered as a constant, noted $\dot{z}_j$ and pulled out of this integral: this yields to the expression 6:

$$p = \frac{2.n_e.n_o}{\lambda}\sum_{j=0}^{p-1}\left[\dot{z}_j\left(\int_{\theta_j}^{\theta_{j+1}} \frac{\sqrt{g^2(\theta)-k_p^2}}{g^2(\theta)}d\theta\right)\right] \qquad 6$$

The integral now only depends on θ and can be calculated. It is noted $I_{j,p}$ and the relation 6 writes down:

$$p = \frac{2.n_e.n_o}{\lambda}\sum_{j=0}^{p-1}\left[\dot{z}_j.I_{j,p}\right] \qquad 7$$

Applying now this relation to the first extremum, the second and so on up to the p^{th} extremum, a linear system is obtained:

$$\begin{aligned}
&\frac{1.\lambda}{2.n_e.n_o} = \dot{z}_0.I_{0,1}\\
&\frac{2.\lambda}{2.n_e.n_o} = \dot{z}_0.I_{0,2} + \dot{z}_1.I_{1,2}\\
&\vdots\\
&\vdots\\
&\frac{p.\lambda}{2.n_e.n_o} = \dot{z}_0.I_{0,p} + \ldots + \dot{z}_{p-1}.I_{p-1,p}
\end{aligned} \qquad 8$$

This system can be solved to give the local derivatives $\dot{z}_j$ and consequently the function $\theta(z)$ itself is readily obtained. The required integration constant is the surface tilt angle of

the director and is obtained by measuring the angle of incidence limit between the T.I.R. and the transmission regimes (Ref. 2).

2. RESULTS.

The results presented here concerns the same samples as these studied in the reference 2 where it can be found the temperature change within the pump beam and the surface tilt angle of the director. Here are given the results obtained by processing the TM mode (extraordinary wave) set of reflectivity curves, that is to say the bulk director distribution determination.

A set of reflectivity curves recorded in the center of the pump beam for different pump powers is shown in figure 2.

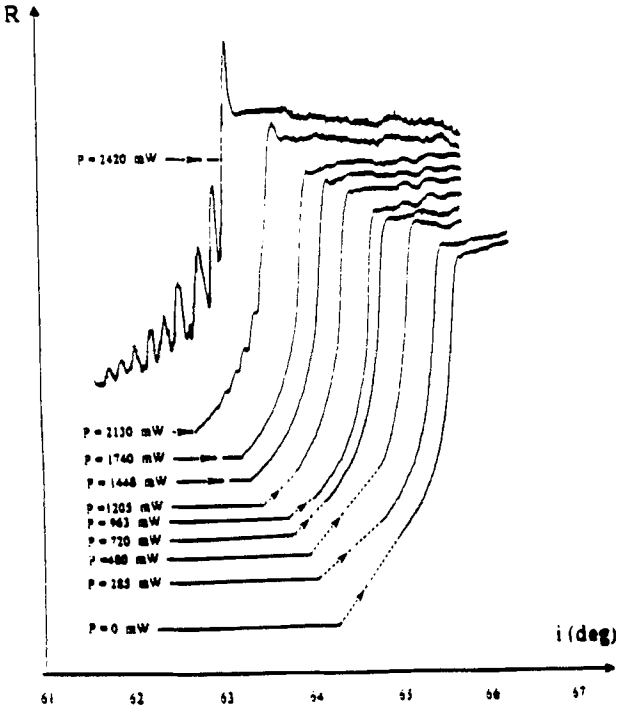

FIGURE 2 TM mode: reflectivity curves recorded at the center of the pump beam for different pump powers.

The interference pattern obtained for the highest power has been processed according to the method described above and the obtained function $\theta(z)$ is shown in figure 3; comparison with theoretical model is underway.

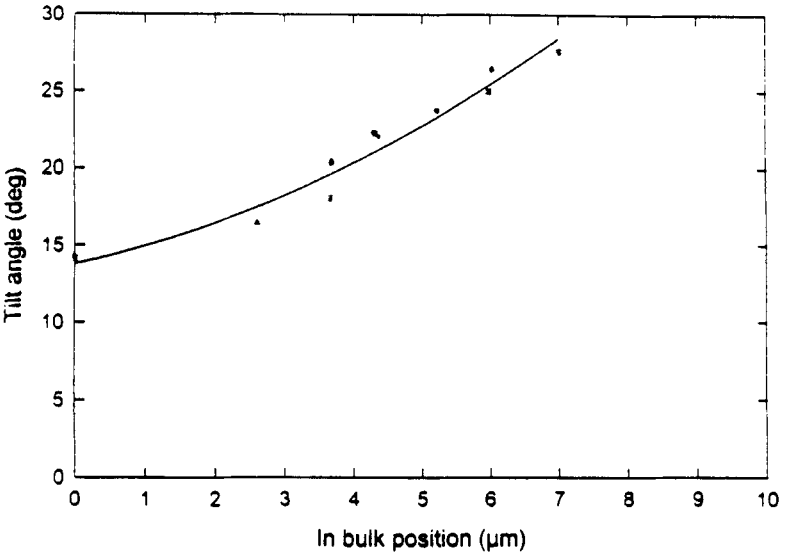

FIGURE 3 Bulk director distribution obtained from the interference pattern processing.

As it can be seen on this curve, the tilt angle is very large: it should be remembered that the sample is around 80μm thick and a value up to 30 degrees is obtained at only 10μm from the boundary. That means that the tilt angle in the middle part of the film should be very large, certainly around 80 degrees.

In addition to these values which concern only the center of the pump beam, in short the function θ(r=0, z), it should be given the radial profile of the distribution θ(r,z). Unfortunately, as it can be seen in figure 2, only one fringe pattern is visible. The actual question that should be asked is not why is there no pattern present in the other curves but why a pattern is observed for a high pump power. Indeed, the distorsion of the nematic induces a distorsion of the front wave of the probe beam reflected within the sample thus preventing the pattern from being onset (Fig. 4a,b). Conversely, a fringe pattern can be observed only in case of a small induced distorsion in the region illuminated by the probe beam (Fig. 4c). In other words, the fringe pattern obtained for a high pump power means that the front wave of the probe beam is no longer distorded in the center region of the pump beam and the reorientation profile (radial dependence of θ(r,z)) should be a flat curve in that region: the profile is much more wider than the pump profile. Another observation goes in the sense of a reorientation profile larger than the pump beam profile: it is the diffraction pattern behavior.

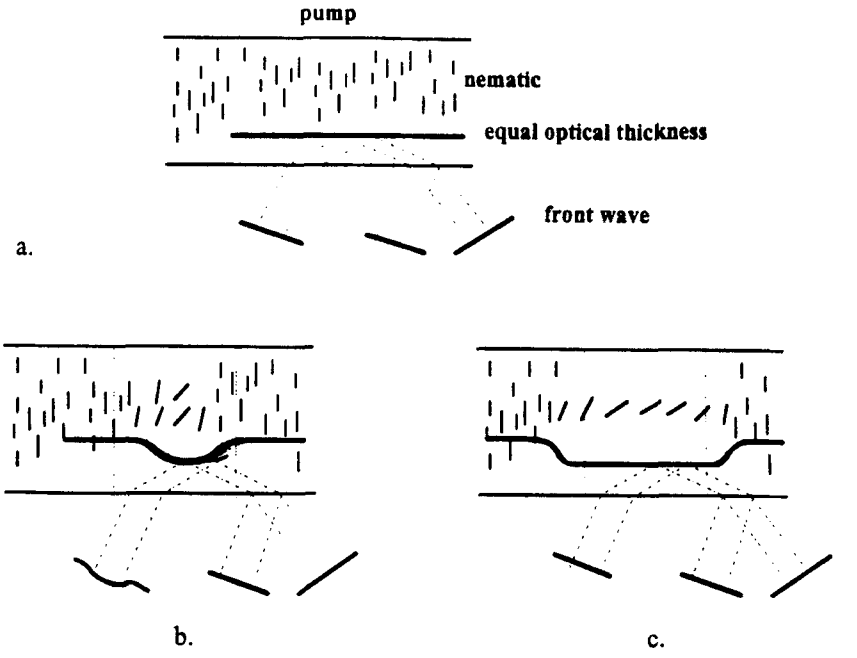

FIGURE 4 Distorsion of the probe beam front wave: the dotted lines indicates the dimensions of the pump beam.
a: unperturbed nematic film; b: low pump power induced distorsion;
c: high pump power induced distorsion.
In the case b, interferences are localised and can not be seen.

3. DIFFRACTION PATTERN STUDY.

The number of rings that have been counted in the far field of the pump beam (3m) is plotted against the pump power (Fig. 5). For the large pump powers, the diffraction regime disappears, the material still being in the nematic phase (cf. Ref. 2). To our knowledge, a decrease of the number of rings has been reported once[3] but such a disappearance has never been reported. As it is explained in the following graphical discussion, it should be a consequence of the weak anchoring conditions.

Roughly speaking, the number of rings N is given by the difference between the local refractive indices of the nematic in the middle ($\bar{n}_a$) and in the edge ($\bar{n}_b$) of the pump beam, both indices being averaged over the thickness e of the film[6]:

$$N = \frac{e}{\lambda}\cdot\left(\bar{n}_a - \bar{n}_b\right) \qquad 9$$

It can be formally decided that the diffraction regime is entered as N is different from zero, that is to say as the index difference is larger than λ/e; in our experiment, larger than 0.006. The main notations that are necessary for our purpose and which describe the distorsion of a nematic film induced by an optical field are depicted in figure 6.

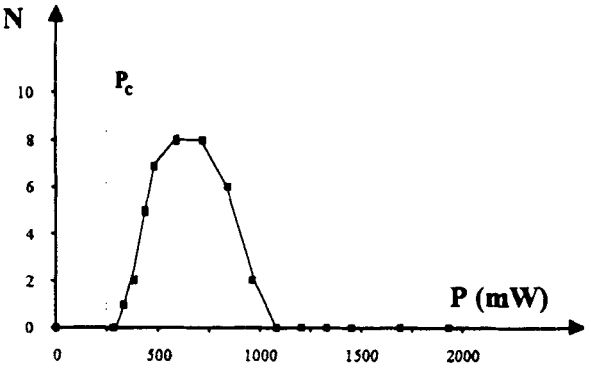

FIGURE 5 Number of diffraction rings versus pump power.

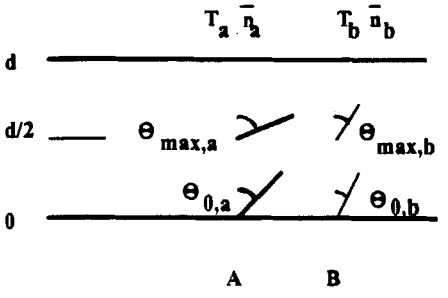

FIGURE 6 Main parameters depicting the optically induced distorsion of a nematic film. A and B corresponds respectively to the center and the edge of the pump beam.

At a distance r from the center of the pump beam, the averaged index is given the expression 10:

$$\bar{n}(r) = \frac{1}{e}\int_0^e n(\theta_{(r,z)}).dz$$

$$n(\theta_{(r,z)}) = \frac{n_e.n_o}{\sqrt{n_e^2\cos^2(\theta)+n_o^2\sin^2(\theta)}} \qquad 10$$

This index depends on the temperature via the principal indices n_e and n_o. With the two points A and B depicted in figure 6 can be associated two representative points on a chart (index versus temperature) noted A and B as well, as shown in figure 7.

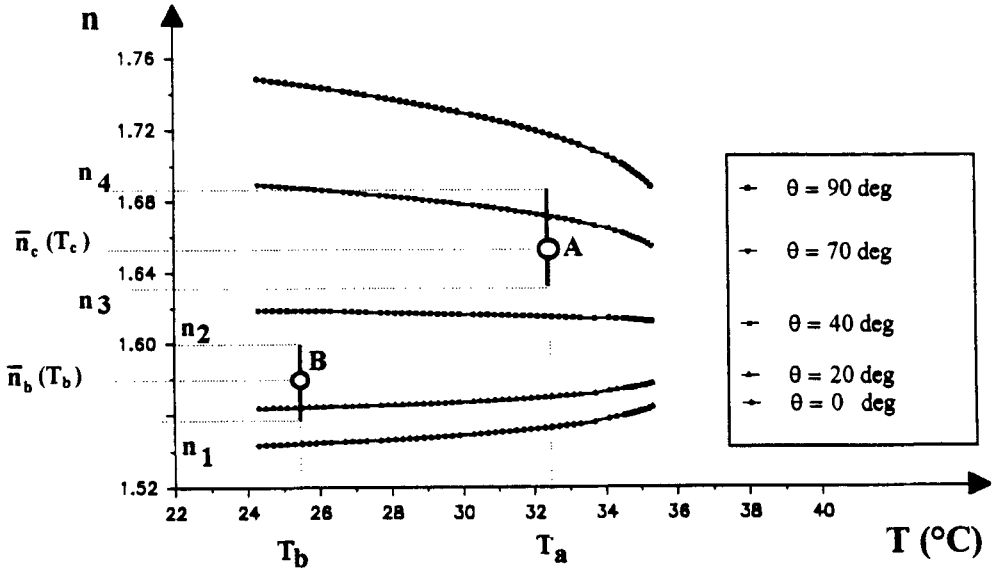

FIGURE 7 Graphic representation of the averaged indices that intervene in the diffraction ring number evaluation. The plotted curves correspond to the 5CB index calculated using the relation 10b for some tilt angle values shown in the inset. The representative points of the edge (B) and the center (A) part of the pump beam being averages, they are respectively in between n_1, n_2 and n_3, n_4 with:
$n_1 = n(\theta_{0,b},T_b)$; $n_2 = n(\theta_{max,b},T_b)$; $n_3 = n(\theta_{0,a},T_a)$; $n_4 = n(\theta_{max,a},T_a)$.

In our experiment, the temperature T_a and T_b can be estimated from the profiles which have been deduced from the TE mode reflectivity curves and discussed in the reference 2: the difference between these temperatures do not exceed 1 or 2 degrees. The

surface tilt angles are also known from this previous paper. Enough parameters are known to start the discussion on the curve shown in figure 5.

Initially the sample is homeotropic and both points A and B are at the same place on the chart (point C on the lower curve, ordinary index, Fig. 8a). As the pump power is increasing, the temperature in the middle and in the edge increases: the points A and B shift to the right. In addition, in the center, the reorientation occurs, shifting up the point A: the difference between both indices $\overline{n_a}$ and $\overline{n_b}$ is no longer zero and the film is focusing. As this difference is larger than 0.006, the diffraction regime is entered. The maximum ring number is attained as the index difference is maximum: the reorientation in the center must be very large compared with that of the edge; in other words, the maximum is attained as the reorientation profile is just a bit narrower than the pump beam profile. In addition, the surface tilt angle being no longer zero at the center, the lowest value (n_3, Fig. 7) permitted for $\overline{n_a}$ is larger than the ordinary index $n_o(T_b)$, as a result, the point A can shift up "more easily". The temperature slightly intervenes in that process. Now as the power is still increasing, the number of rings decreases: on such a chart (Fig. 7), that means that the y-axis distance AB is decreasing. Physically, the point A cannot shift down because the reorientation is obviously increasing with the pump power, therefore it is the point B that shifts up. This is possible if at least $\theta_{max,b}$ increases and also if both angles $\theta_{0,b}$ and $\theta_{max,b}$ increase. Thus the ring number decrease can be explained in saying that the reorientation in the center of the pump beam saturates (tilt angle close to 90 degrees) and the representative point A do not move a lot on the chart, whereas in the edge, the reorientation is still increasing lifting up the point B (Fig. 8c). In other words, for such large pump powers, the reorientation profile is certainly wider than the pump beam profile. Still increasing the power, the reorientation profile becomes wider and wider, the point B lifts up to be very close to A and the diffraction regime disappears as the y-axis AB distance is smaller than 0.006: the film is again focusing and for higher pump powers it can become defocusing, should the point B be upper than A (Fig. 8d). The point B close to the point A on such a chart means that the lower and higher values (n_1, n_2, Fig. 7) limiting $\overline{n_b}$ must be very large in other words the tilt angles on the interface and in the middle part of the film must be large. To obtain the point B higher than the point A, it is necessary that these angles are around 70 or 80 degrees at least for the 5CB material. Considering the interface tilt angles, such large values can be achieved only in case of very weak anchoring conditions. Such a focusing-defocusing sequence has been observed with the sample 2 (cf Ref. 2) which exhibits a surface tilt angle that increases linearly with the pump power, this increasing starting from very small pump power which is a weak anchoring signature. Moreover, this focusing-defocusing sequence has not been observed with the other reported sample

(sample 1, Ref. 2) the surface tilt angle of which exhibits a thresholdlike behavior. It is worth noticing that the defocusing capability of the film is due to thermal contribution only, given that the tilt angle in the center of the pump beam is certainly larger than on the edge, the point A is on a curve associated with a tilt angle larger than that of the point B as a result B can be higher than A only due to a lower temperature.

CONCLUSION

In this paper, has been reported measurements and observations on the photorefractivity of a nematic film. An Argon laser beam illuminates a homeotropically aligned nematic film under normal incidence. The boundary conditions for the film are weak. By processing the interference pattern that occurs between the part of the probe beam reflected on the nematic boundary and the part reflected within the nematic volume, it has been possible to obtain the director tilt angle distribution at the center of the pump beam as a function of the distance from the interface. A very large optically induced reorientation has been found: up to 80 degrees in the middle part of the sample. This numerical value is valid for the used material, 5CB. In addition, from the observation of the diffraction ring pattern, it has been deduced that one of the films exhibits a sequence focusing-diffracting-focusing-defocusing as the pump power is increased. A graphical discussion is proposed to show that the weak anchoring conditions enable this behavior and the defocusing in this sequence is a pure thermal effect.

REFERENCES

1. For example:
R. M. Herman and R. J. Serinko, Phys. Rev. A., 19,1757,(1979).
R. M. Herman and R. J. Serinko, Phys. Rev. A., 19,1757,(1979)
A. S. Zolot'ko, V. F. Kitaeva, N. Kroo, N.N. Sobolev and L. Chillag, JETP. Lett., 32, 158, (1980).
A. S. Zolot'ko, V. F. Kitaeva, N. N. Sobolev and L. Chillag, JETP. Lett.,32 (2), 158, (1980).
I. C. Khoo and S. L. Zhuang, Appl. Phys. Lett., 37, 3, (1980).
N. V. Tabiryan and B. Ya Zel'dovich, Mol. Cryst. Liq. Cryst., 62, 237,(1981); Mol. Cryst. Liq. Cryst., 69, 19, (1981); Mol. Cryst. Liq. Cryst., 69, 31, (1981).
I. C. Khoo, S. L. Zhuang and S. Shepard, Appl. Phys. Lett., 39(12), 937, (1981).
N. V. Tabiryan, A. V. Shukov and B. Y. Zel'dovich, Mol. Cryst. Liq.Cryst., 136, 1, (1986).
I. C. Khoo, Prog. in Optics, XXVI, 105, (1988).

2. M. Warenghem, M. Ismaili, F. Simoni, F. Bloisi, L. Vicari, This issue.
3. F. Bloisi, L. Vicari, F. Simoni, G. Cipparone and C. Umeton, JOSA B, 12, 2462, (1988).
4. F. Bloisi, L. Vicari and F. Simoni, Mol. Cryst. Liq. Cryst., 179, 45, (1990).
5. F. Simoni, F. Bloisi, L. Vicari, M. Warenghem, M. Ismaili and D. Hector, EUROPHYS. Lett., 21(2), 189, (1993).
6. S.D. Durbin, S.M. Arakelian and Y.R. Shen, Opt. Lett., 6(9), 411, (1981).